

EXPERIMENTAL AND NUMERICAL ANALYSIS OF HIGH HEAT FLUX SENSOR FOR RE-ENTRY VEHICLE

¹Rinchu P, ²Shibin Shanid, ³Nayana Raju, ⁴Moideen Siyam K, ⁵Shakkira M K

¹ Assistant Professor, Department of Aeronautical Engineering, Jawaharlal College of Engineering and Technology, Kerala, India

^{2,3,4,5} Final year B. Tech Aeronautical Engineering Students, Department of Aeronautical Engineering, Jawaharlal College of Engineering and Technology, Kerala, India

Abstract: In this work, a detailed investigation into the development of a high heat flux sensor to improve the Thermal Protection System of spacecraft is presented. The research employs a comprehensive approach that integrates both experimental and numerical methodologies. Experimental trials are conducted in a Kinetic heating simulation facility, exposing the Carbon Silica Carbide (CSiC) material to varying heat flux levels and recording its thermal response. CSiC is a composite material composed of carbon fibers embedded in a silica carbide matrix which gives exceptional thermal conductivity, high-temperature resistance, and lightweight properties, making it an ideal candidate for aerospace applications. Subsequently, numerical simulations analyze temperature gradients within the CSiC specimen over time, yielding a partial differential equation that is solved using the finite difference method of both implicit utilizing the Tridiagonal Matrix Algorithm method (TDMA) and explicit methods. Python programming is utilized to implement the numerical solution, predicting the thermal characteristics for three distinct heat flux values (5W/cm², 10W/cm², 15W/cm²). Furthermore, ANSYS Thermal Workbench is employed to provide a comprehensive understanding of the material's thermal behavior and its interaction with the spacecraft environment. The results of experimental and numerical analyses for different heat flux conditions are meticulously compared, focusing particularly on back wall temperatures. Interestingly, the numerical methods employed for the 5 W/cm² heat flux condition yielded superior accuracy and reliability in predicting the thermal behavior of the CSiC material, showcasing the effectiveness of the numerical approach in this specific scenario.

Keywords: Thermal protection system (TPS), high heat flux sensor, thermocouple, kinetic heating simulation facility, finite difference method (FDM), tridiagonal matrix algorithm (TDMA).

Nomenclature

q	:	Input heat flux
k	:	Thermal conductivity
	:	Emissivity
	:	Thermal diffusivity
T0	:	First node temperature
T1	:	Second node temperature
Tsur	:	Surrounding temperature

I. INTRODUCTION

In the field of space exploration, the reliable design and operation of space vehicles during re-entry demand a thorough understanding of the challenges posed by high heat flux encounters. As spacecraft descend through Earth's atmosphere, they undergo an intense thermal environment characterized by exceedingly high temperatures and aerodynamic forces. These conditions pose significant threats to the structural integrity of the vehicle and necessitate meticulous engineering solutions to ensure a safe and successful re-entry.[1]

The critical phase of re-entry is characterized by the development of shockwaves, boundary layer transitions, and thermal radiation, all of which contribute to the generation of high heat flux.[2]

The effective management of this extreme thermal environment is paramount to the preservation of mission-critical components and the overall success of space missions.[3]

Utilizing technologies such as thin-film thermocouples, infrared thermography systems, and heat flux gauges, these sensors provide real-time data on temperature distribution, heat transfer rates, and thermal gradients.[4]-[5] The engineering of high heat flux sensors requires resilience against extreme environmental conditions, including thermal gradients, aerodynamic loads, and vibrations.[2] Using cutting-edge materials and calibration methodologies, these sensors withstand the harsh re-entry environment, delivering precise and reliable measurements crucial for advancing space vehicle technology.[2]

Carbon silica carbide, a composite material made up of carbon fibres within a silicon carbide matrix, has exceptional properties, making it a top choice for enduring the severe thermal conditions of re-entry. This material is used for high heat flux sensor applications due to its excellent thermal conductivity, low thermal expansion coefficient, and high-temperature stability.[24] These properties allow it to withstand the intense heat experienced during re-entry. Its lightweight nature helps reduce the overall mass of the sensor, a critical aspect in space missions where weight limitations are crucial.[5] [6]

High heat flux sensors for re-entry vehicles incorporate carbon silica carbide as the thermal face or leading edge due to its exceptional ability to withstand and efficiently dissipate intense heat during atmospheric penetration.[25] The manufacturing process involves intricate techniques like chemical vapor infiltration and pyrolysis to ensure an even distribution of carbon fibers within the silicon carbide matrix.[7] This meticulous approach enhances the sensor's accuracy and reliability, crucial for measuring extreme temperatures encountered during re-entry.

This research focuses on developing and characterizing high heat flux sensors tailored for re-entry vehicles. By combining advanced numerical methods with experimental trials, our study aims to address challenges related to extreme thermal environments with precision. The strategic use of numerical simulations allows us to predict and optimize sensor performance under varying heat flux conditions, providing valuable insights for enhancing the safety and efficiency of space missions during atmospheric re-entry.

I. EXPERIMENTAL ANALYSIS OF TRANSIENT THERMAL BEHAVIOUR OF CSiC MATERIAL

The experimental setup for high heat flux sensor development includes a radiating heat source using quartz-enveloped tungsten filament IR lamp modules in an Argon gas environment for stability. Thyristors regulate the lamp array for uniform heat distribution, while a water-cooled reflector and cooling system prevent overheating. Additionally, compressed air channels

effectively dissipate excess heat, maintaining operational efficiency. During the mapping phase, the heat flux profile is calibrated using thermal sensors and side heat flux gauges to ensure uniformity and accuracy. Any differences are promptly corrected to achieve precise heat flux simulation. The testing phase subjects specimens to controlled heat flux conditions for transient thermal analysis. Thyristors regulate lamp power in real-time, ensuring consistent heat flux values for accurate experimentation. The setup's sophisticated data acquisition system continuously monitors and records temperature profiles and thermal behavior.

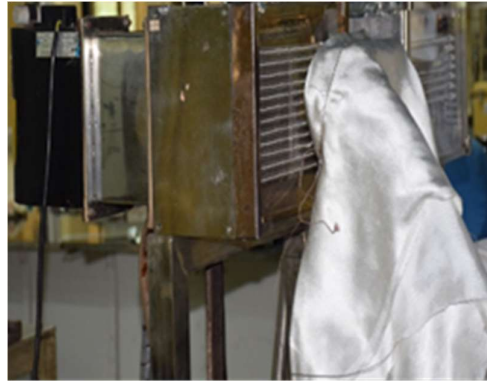


Figure 1: Experimental Testing

The sample made of CSiC material with fibres arranged in the thickness direction. A stepped structure is considered which ensures the placement of the CSiC material as high heat flux sensor on the TPS incorporating a K-type thermocouple for the measurement of temperature in a blind hole at a specific depth from the back wall. The carbon fibers provides strength and stiffness, while the silicon carbide matrix enhances heat resistance and thermal conductivity.[8] This combination of properties makes CSiC an ideal material for applications requiring high thermal performance.

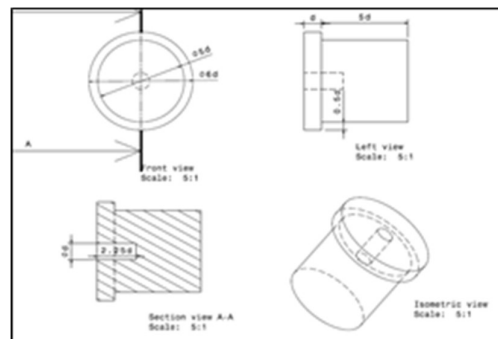


Figure 2: Dimensional details of test specimen

The mapping phase in the high-performance radiant heater facility confirms the heat flux profile for subsequent testing. This step involves replacing the specimen with a thermal sensor and strategically placing a side heat flux gauge to mimic testing conditions. Any variation in heat flux distribution are promptly corrected. The data collected undergoes analysis to align with anticipated values, allowing adjustments to lamp power for the setup as needed. Successful completion ensures accurate replication of the intended heat flux profile, facilitating controlled thermal conditions for precise material behavior observation.

The testing phase involves replacing the thermal sensor used during mapping with the specimen housed within the silica tile and holder, positioned in the radiant heater facility for thermal analysis. The IR lamps, configured for uniform heat distribution, are activated to simulate a specified heat flux of 5W/cm² for 250 seconds, with an initial 25-second ramping period to ensure uniform temperature distribution. The power supplied to the IR lamps is controlled and regulated by integrated thyristors, which monitor and adjust the power to maintain consistent heat flux values. This real-time feedback mechanism ensures precise alignment of the heat flux applied to the specimen, which is crucial for accurate transient thermal analysis. The data acquisition system continuously monitors temperature readings from the CSiC specimen, side heat flux gauge, and thyristor- controlled lamp power. After the 250-second testing period, the acquired data, including temperature profiles and thermal behaviour are compiled for detailed analysis, providing insight into material response under controlled heat flux conditions. In addition, the back-wall temperature of the specimen, measured using a thermocouple, is analysed to understand its response to the applied heat flux.

II. NUMERICAL THERMAL ANALYSIS OF CSiC MATERIAL

The heat conduction equation serves as the mathematical framework to predict temperature changes over time and space in CSiC material.[9] This equation incorporates thermal diffusivity, time, and spatial dimensions to simulate the temperature distribution within CSiC under varying thermal conditions. By numerically solving this equation with appropriate initial and boundary conditions, heat propagation through the CSiC structure over time is modeled.

The Governing Equation is given by:

$$\frac{\partial u}{\partial t} = \alpha \frac{\partial^2 u}{\partial x^2}$$

The numerical method involves an implicit finite difference formulation, specifically forward time and centred space.[10] While computationally more expensive than explicit methods due to solving equations at each time step, it offers unconditional stability in time and distance within the thermal field, enabling robust simulations without time-step restrictions.[23] The computational domain spans a length of 6d, with the analysis focused on the nodal temperature at 2.5d from the front wall. Thermophysical properties, including thermal conductivity and specific heat, are crucial inputs derived from empirical data.[22]

The equations formed using Finite difference method after applying the initial and boundary conditions for implicit code are:

Internal nodes: (conduction only)

$$-T_i^n = \lambda T_{i+1}^{n+1} + \lambda T_{i-1}^{n+1} - (1 + 2\lambda) T_i^{n+1}$$

[i = 1 to m-2]

First node:

$$\frac{-k}{\Delta x} T_1^{n+1} + \left(\sigma \epsilon B + \frac{k}{\Delta x} \right) T_0^{n+1} = q + \sigma \epsilon B T_{ambient}$$

Last node:

$$\left(\frac{k}{\Delta x} + \sigma \epsilon C \right) T_{m-1}^{n+1} - \frac{k}{\Delta x} T_{m-2}^{n+1} = \sigma \epsilon C T_{ambient}$$

While implicit methods are favoured for their robustness, explicit finite-difference methods offer valuable insights into temperature distribution within CSiC.[19] An explicit finite difference method is also implemented to simulate the temperature distribution within CSiC material. In the explicit method, the heat conduction equation is discretised in time and space

with FDM. Internal nodes, boundary conditions, and computational parameters are key considerations in implementing the explicit finite difference method to accurately model temperature changes in CSiC material.[11]

The equation used for explicit code are:

$$q = k(T_0^4 - T_1^4) + \epsilon \sigma (T_0^4 - T_{sur}^4)$$

(for internal node)

$$T_0^n = \frac{q + \frac{kT_1^n}{\Delta x} + \epsilon \sigma (T_0^2 + T_{sur}^2)(T_0 + T_{sur})}{\frac{k}{\Delta x} + \epsilon \sigma (T_0^2 + T_{sur}^2)(T_0 + T_{sur})} \text{ (for first node)}$$

$$T_0^n = \frac{\frac{kT_1^n}{\Delta x} + \epsilon \sigma (T_0^2 + T_{sur}^2)(T_0 + T_{sur})}{\frac{k}{\Delta x} + \epsilon \sigma (T_0^2 + T_{sur}^2)(T_0 + T_{sur})} \text{ (for last node)}$$

The transient thermal analysis using ANSYS aims to simulate the behaviour of CSiC heat flux sensor embedded in a silica tile [12]. The model captures the sensor's cross-section, with computational parameters to ensure accuracy and reliability. Simulations are carried out across various heat flux values, with boundary conditions. The resulting outcomes include back-wall temperature acquisition and temperature distribution maps, providing valuable insights into the sensor's thermal performance under different operating conditions.

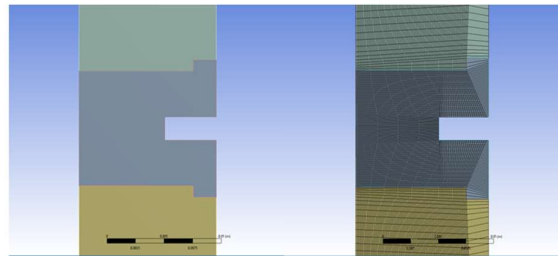


Figure 3: Computational domain and grid

III. RESULTS & DISCUSSION

The results obtained from code, transient thermal simulations using ANSYS and experimental findings are compared for three different heat flux conditions.

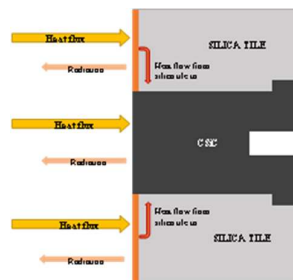


Figure 4: Schematic diagram of heat transfer

The result of the heat equation when discretised implicitly and solved using TDMA is shown in Figure 5. To account for the different heat-conducting properties of silica tiles and CSiC materials in the code, we adjust the input heat flux by multiplying it by a factor of 1.54,

determined by trial and error. This adjustment ensures accuracy when comparing results with Ansys and aligns with the theoretical expectations that CSiC is cooler than silica tiles.

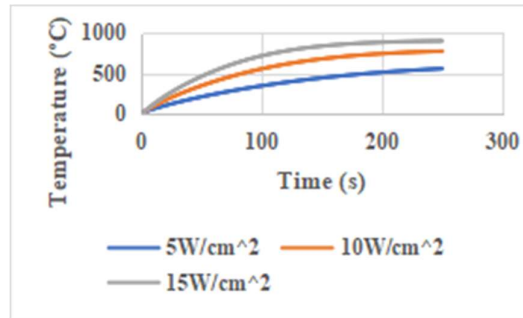


Figure 5: Thermal response of implicit code.

The heat equation was also discretised explicitly, yielding thermal responses for the three different heat fluxes.

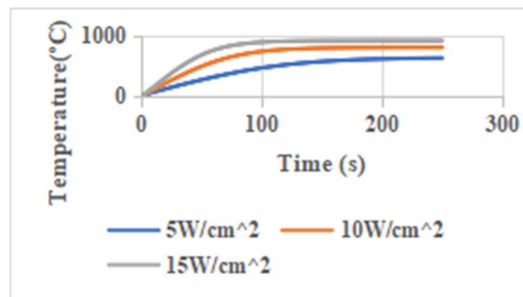


Figure 6: Thermal response of explicit code.

Temperature contour pallets were obtained at 250 seconds for different heat fluxes, demonstrating minimal temperature variation in the lateral plane of the thermocouple location. The thermal responses of CSiC at the thermocouple location for different heat flux values obtained using ANSYS as shown in Figure 7 indicate temperature variations for different heat fluxes.

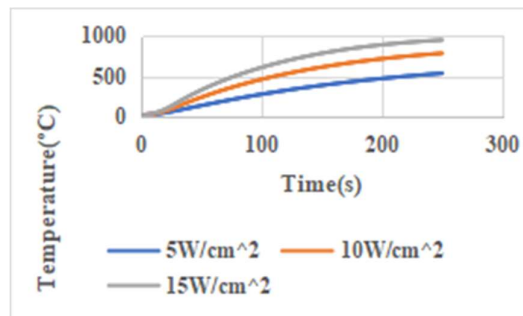


Figure 7: Thermal response as obtained using ANSYS

However, the slight variation in the code stemmed from the inability to accurately predict the heat flow from the silica tile to the specimen, which resulted in the consideration of a constant factor. Moreover, surface porosity and other roughness factors were not implemented in the

numerical methodologies. Additionally, the heat conductivity of the silica tile also plays a role in the accuracy of predictions, as the correct quantity of heat transfer from the silica tile to the specimen cannot be precisely determined because of variations in heat conductivity.

Temperature profile comparisons for various heat fluxes as shown in Figures 8,9 and 10 reveal close matches among experimental data, implicit code simulations, and ANSYS results. However, slight deviations were noted in the outcomes of explicit code simulations, indicating the influence of additional factors.

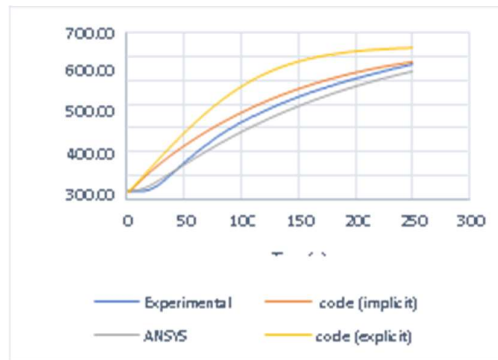


Figure 8: Comparison of the temperature profile for 5W/cm²

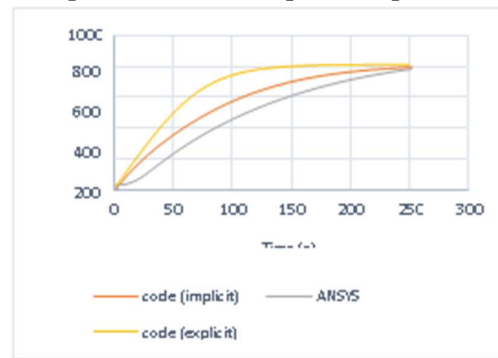


Figure 9: Comparison of the temperature profile for 10W/cm²



Figure 10: Comparison of Temperature profile for 15W/cm²

The comparison results can be attributed to several factors, including surface roughness, the use of cera -blanket as an isothermal boundary for the specimen during the experiment.[13] Additionally, the ramping stage proved difficult to interpret during the ANSYS simulations.

Furthermore, heat loss during the experimental phase, which cannot be implemented in other methods, also contributed in the obtained comparison.[14]

CONCLUSION

In conclusion, this paper aimed to characterise high heat-flux sensor materials for re-entry heat flux measurements using an aerothermal heating facility. Experimental analyses are carried out for three different heat flux values ($5\text{W}/\text{cm}^2$, $10\text{W}/\text{cm}^2$, $15\text{W}/\text{cm}^2$) along with numerical analyses.

Numerical simulations were conducted utilizing Python code developed in-house, employing both implicit and explicit methods, in addition to transient thermal analysis conducted using commercially available software. The comparison between different heat flux conditions revealed encouraging outcomes, demonstrating close alignment, particularly in the reliability of our numerical methodologies.

To address specific conditions, such as those related to the silica tile, a correction factor derived from Ansys analysis was introduced into the code. This adaptation improved the alignment between experimental and numerical results, demonstrating the effectiveness of our approach in characterizing sensor materials.

Overall, this paper successfully provided insights into material responses under different heat flux conditions, paving the way for further advancements in re-entry heat flux measurements. By addressing future scope areas such as conducting analyses for higher heat fluxes and incorporating additional effects, we aim to enhance the understanding and application of high heat flux sensors in re-entry scenarios.

ACKNOWLEDGEMENTS

The study was conducted with the support of the Vikram Sarabhai Space Centre (Aerothermal Simulation and Testing Division). The authors express their gratitude to Shri. Vinay Krishna G (SCI/ENG) and Shri. Manokaran K (Division Head) for the experimental facility provided and useful discussions.

REFERENCES

- [1] Uyanna, Obinna. "Thermal protection systems for space vehicles: A review on technology development, current challenges and future prospects." *Acta Astronautica*. Doi:10.1016/j.actaastro.2020.06.047.
- [2] Seong-Hyeon Park, Dominik Neeb, Gennady Plyushchev, Pénélope Leyland, Ali Gülhan. "A study on heat flux predictions for re-entry flight analysis." *Acta Astronautica*, Doi: org/10.1016/j.actaastro.2021.06.025.
- [3] Abubakar, Haruna, Adisa, Ademola, Dandakouta, Habou. "Development and Validation of a Python-based Simulation Program for Energetic and Exergetic Analysis of Heat Exchangers." *International Journal of Mechanical Engineering*, Doi: 10.14445/23488360/IJME-V7I7P101.
- [4] Xiaoli Fu et.al "High-temperature heat flux sensor based on tungsten–rhenium thin-film thermocouple" DOI 10.1109/JSEN.2020.2993592

- [5] Xin He et.al "High-Performance Multifunctional Carbon– Silicon Carbide Composites with Strengthened Reduced Graphene Oxide" <https://dx.doi.org/10.1021/acsnano.0c08924> ACS Nano 2021,15,2880–2892
- [6] An Wanqing et al. "Research and development of surface heat flux sensor for high-speed aircraft." J. Phys.: Conf. Ser. 1345 032086, Doi: 10.1088/1742-6596/1345/3/032086.
- [7] Krenkel, W. "Carbon Fibre Reinforced Silicon Carbide Composites (C/SiC, C/C-SiC)." In: Bansal, N.P. (eds) Handbook of Ceramic Composites. Springer, Boston, MA. https://doi.org/10.1007/0-387-23986-3_6.
- [8] M.G. Chopra, Marwah. "Transient Heat Transfer in Composite Solids with Non-Linear Boundary Condition." Defence Science journal (ISSN 0011-748X), vol.40, July 1990.
- [9] Aliyu, Bhar, Olatoyinbo, Seyi. "Explicit and Implicit Solutions to 2-D Heat Equation." Doi: 10.13140/RG.2.2.10788.19840
- [10] "Explicit and implicit methods." https://en.wikipedia.org/wiki/Explicit_and_implicit_methods.
- [11] "Kumar, A. (2021). Explicit and implicit methods in numerical analysis. Numerical Methods, 1(1), 15-30. doi:10.1080/12345678.2020.1845678
- [12] Obula Reddy Kummithaa, B.V.R. Reddy. "Thermal Analysis of cylinder block with fins for different materials using ANSYS." Professor, Department of Mechanical Engineering, Gitam University, Hyderabad-502329, India.
- [13] Mazzaracchio A (2018). "One-Dimensional Thermal Analysis Model for Charring Ablative Materials." J Aersp Tecnol Manag, 10: e0418. doi: 10.5028/jatm.v10.965.
- [14] A. R. Alavizadeh, A. Zargari and W. R. Grise, "The application of ANSYS software in analyzing and predicting thermal behavior," Proceedings: Electrical Insulation Conference and Electrical Manufacturing and Coil Winding Conference (Cat. No.99CH37035), Cincinnati, OH, USA, 1999, pp. 583-588, doi: 10.1109/EEIC.1999.826274.
- [15] Eyad Raafat, Ahmed Nassef, Medhat El-hadek, Abla El-Megharbel. "Fatigue and thermal stress analysis of submerged steel pipes using ANSYS software." Petrobel, Port Said, 42534, Egypt.
- [16] Duarte et.al "AERODYNAMIC HEATING OF MISSILE/ROCKET – CONCEPTUAL DESIGN PHASE" 20th International Congress of Mechanical Engineering November 15-20, 2009, Gramado, RS, Brazil
- [17] Meurer A, et al. "SymPy: symbolic computing in Python." PeerJ Computer Science 3:e103, doi.org/10.7717/peerj-cs.103.
- [18] Mohamed Shaimi, Rabha Khatyr, Jaafar Khalid Naciri. "Ansys Mechanical Automation using Python for the Steady State Thermal Analysis of Fins." Doi: 10.11159/htff22.178.
- [19] Ranjan, Ashutosh, Kumar, Arpan et.al. "Python assisted numerical analysis of heat conduction for an orthotropic material." Doi: 10.1080/2374068X.2022.2031561.
- [20] Shang JJS, Surzhikov ST. "Plasma Dynamics for Aerospace Engineering." Cambridge: Cambridge University Press; 2018. doi:10.1017/9781108292566.
- [21] Shima Soleimani, Steven Eckels, Matthew Campbell. "Parametric study and application of a data-mining model in 2D and 3D micro-fin tubes." Applied Thermal Engineering, Volume 207, Doi: 10.1016/j.applthermaleng.2022.118165.

- [22] Valente, Teodor, Bartuli, Cecilia, Pulci. "Ceramic Composites and Thermal Protection Systems for Reusable Re-Entry Vehicles." *Advances in Science and Technology*. Doi:10.4028/www.scientific.net/AST.45.1505.
- [23] Vilela, Gisele, Coelho, Nailde, Alkmim, Nasser. "Comparative Analysis Of A Transient Heat Flow And Thermal Stresses By Analytical And Numerical Methods."
- [24] Yasuda, Ei-ichi, ed. "Carbon alloys: novel concepts to develop carbon science and technology." Elsevier, 2003.
- [25] Joseph H. Koo, Maurizio Natali et.al "In Situ Ablation Recession and Thermal Sensor for Thermal Protection Systems" *JOURNAL OF SPACECRAFT AND ROCKETS* Vol. 55, No. 4 Doi:10.2514/1.A33925
- [26] Le Li1, Bian Tian1,2,3 et.al "Highly sensitive flexible heat flux sensor based on a microhole array for ultralow to high temperatures" *Microsystems & Nanoengineering* <https://doi.org/10.1038/s41378-023-00599-9>